reduction and improved stability[16,17]. The Wendelstein 7-X (W7-X) stellarator in Greifswald, Germany has just begun operation[18]; the 3D magnetic field was optimized computationally to reduce the loss of heat due to collisional processes. The results are already interesting. All efforts would be helped by higher magnetic fields (see for example ref. 19) and several countries are running active programmes for the development of high-temperature high-field superconducting magnets, but these are not yet available at a useful scale.

Fusion is not ready for the market, but we are close enough to see the final challenging steps. We must make those steps. ❒

Steven C. Cowley is at the Culham Centre for Fusion Energy, Abingdon OX14 3DB, UK and at the Department of Physics, Imperial College, Prince Consort Road, London SW7 2BZ, UK. e-mail: steve.cowley@imperial.ac.uk

References

1. Eddington, A. S. *Nature* **106,** 14–20 (1920).
2. Dawson, J. D. in *Fusion* (ed. Teller, E.) Ch. 16. (Academic Press, 1981).
3. *Lithium* (United States Geological Survey, 2016); http://go.nature.com/CG6i5Y
4. Gilbert, M. R. *et al. Nucl. Fusion* **52,** 083019 (2012).
5. Knaster, J., Moeslang, A. & Muroga, T. *Nature Phys.* **12,** 424–434 (2016).
6. van der Schaaf, B. *et al. Fusion Eng. Design* **69,** 197–203 (2003).
7. Petrizzi, L., Batistoni, P. & Pillon, M. *Fusion Eng. Design* **69,** 593–599 (2003).
8. Maisonnier, D. *et al. Nucl. Fusion* **47,** 1524–1532 (2007).
9. Ongena, J., Koch, R., Wolf, R. & Zohm, H. *Nature Phys.* **12,** 398–410 (2016).
10. Betti, R. & Hurricane, O. A. *Nature Phys.* **12,** 435–448 (2016).
11. Fasoli, A. *et al. Nature Phys.* **12,** 411–423 (2016).
12. https://www.iter.org
13. Shimada, M. *et al. Nucl. Fusion* **47,** S1–S17 (2007).
14. *Fusion Electricity: A Roadmap to the Realisation of Fusion Energy* (EFDA, 2012); http://go.nature.com/7qFq56
15. Zinkle, S. J. & Was, G. S. *Acta Materialia* **61,** 735–758 (2013).
16. Ono, M. & Kaita, R. *Phys. Plasmas* **22,** 040501 (2015).
17. Meyer, H. *et al. Nucl. Fusion* **53,** 104008 (2013).
18. Milch, I. Wendelstein 7-X fusion device produces its first hydrogen plasma. *Max-Planck-Institut für Plasmaphysik* (3 February 2016); http://go.nature.com/2eiEBj
19. Sorbom, B. N. *et al. Fusion Eng. Design* **100,** 378–405 (2015).
20. *Annual Statistical Bulletin 2010/2011* (OPEC, 2011); http://go.nature.com/54jJP2
21. *Natural Gas Proved Reserves* (CIA World Factbook, accessed 10 February 2016); http://go.nature.com/dPb25O
22. *Coal Energy Resources* (World Energy Council, accessed 10 February 2016); http://go.nature.com/gpEzch
23. *Supply of Uranium* (World Nuclear Association, accessed 10 February 2016); http://go.nature.com/Men4OF

Applied and fundamental aspects of fusion science

Alexander V. Melnikov

Fusion research is driven by the applied goal of energy production from fusion reactions. There is, however, a wealth of fundamental physics to be discovered and studied along the way. This Commentary discusses selected developments in diagnostics and present-day research topics in high-temperature plasma physics.

In the wake of the Second World War, several nations — notably the United Kingdom, the USSR and the United States — developed research programmes on controlled thermonuclear fusion with the aim of energy production. The main technical problems to overcome were confining the fusion plasma efficiently and achieving sufficient heating for fusion reactions to happen. Different lines of research were followed — initially largely independently by each nation, as fusion research was formally classified until 1956 in the USSR and 1958 in the UK and US — but by 1968, the tokamak (a Russian acronym for 'toroidal chamber with magnetic coils') had emerged as the most promising route to controlled fusion: the T-3A tokamak (Fig. 1) at the Kurchatov Institute of Atomic Energy in Moscow (then USSR) achieved a plasma temperature of 10 million degrees Celsius, a confinement time of 10 milliseconds and production of thermonuclear neutrons.

The original tokamak concept — a toroidal vessel holding a plasma that acts as the secondary winding of a transformer, created and sustained by the combination of the plasma current and an additional

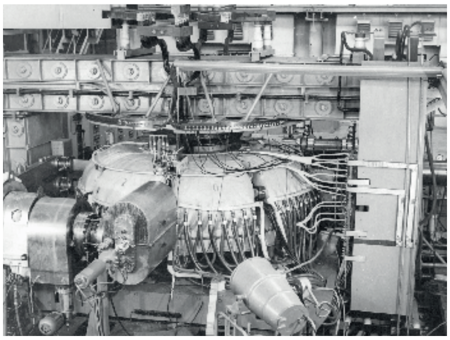

Figure 1 | The T-3A tokamak at the Kurchatov Institute of Atomic Energy. Photograph taken around 1967; reproduced with permission from the NRC 'Kurchatov Institute'.

toroidal magnetic field so that the field lines of the total magnetic field describe helical paths within the torus — goes back to Igor Tamm and Andrei Sakharov, both involved in the Soviet Union's thermonuclear bomb programme. The strongest competitor to the tokamak is the stellarator, which produces the desired helical magnetic field by means of external windings, avoiding the intrinsic problem of tokamaks caused by the plasma current: magnetohydrodynamic instabilities. (For a review of tokamak and stellarator physics, see ref. 1.)

After realization of the first tokamak in 1955, its design was improved step by step[2]. Important improvements developed in the Kurchatov Institute were, for example, the use of an iron core for the tokamak transformer, the use of control coils instead of a copper casing, the change from a circular to an elongated toroidal cross-section and the use of superconducting instead of copper coils.

After 1969, when a British scientific delegation had brought their state-of-the-art equipment from Culham to Moscow to double-check the temperatures generated in T-3A (ref. 3), tokamaks started to be built outside the Soviet Union. Mastering tokamak technology and pursuing magnetic confinement fusion quickly became major international research endeavours. The experience and knowledge accumulated over the past decades have culminated in the design of ITER, the largest ever tokamak, now being built in the south of France[4]. The evolution of tokamak design shows how an applied-physics goal sparked fundamental discoveries in plasma physics, and how the two drive each other forward — as this Commentary aims to demonstrate by discussing a few exemplary cases.

Applied and fundamental fusion research

The ultimate goal of controlled nuclear fusion has always been the realization of a fusion power reactor, based on which a thermonuclear electrical power station can be built[5]. So, traditionally, fusion is considered an applied-science challenge. As is often the case with applied research, however, this practical challenge has led to several new branches of physics that have now developed into independent areas of fundamental research.

The crux of fusion research is the study of the properties of a hot laboratory plasma — matter at extremely high temperatures. This is a truly challenging endeavour, as temperatures required for fusion lie around 100 million degrees Celsius, which is much higher than any naturally occurring temperature in our Solar System — much higher even than the temperature in the Sun's interior.

The applied and fundamental aspects of nuclear fusion are closely intertwined. On the one hand, the drive for achieving the so-called Lawson criterion, necessary for a self-sustained fusion reaction (the applied aspect), requires reaching ever higher plasma parameters (plasma temperature, density and energy confinement time), and thus advancing further into previously unexplored scientific territory (the fundamental aspect). On the other hand, a systematic study of the properties and processes in hot plasmas is the only way forward for optimizing the mechanisms of confinement and transfer of particles and heat, which is key for the design of a fusion reactor.

An illustrative example of the challenges faced by researchers in the fusion technology and engineering sector is the short distance — of the order of 1 m — between a tokamak plasma, at the highest temperature in our Solar System, and the superconducting coils required for generating the confining magnetic field, at liquid-helium temperature, close to the lowest naturally occurring temperatures in the Universe. A machine capable of dealing with such an enormous temperature gradient requires substantial design efforts combined with research and development on heat- and radiation-resistive materials[6].

Fusion-plasma physics and diagnostics

How can we study a hot plasma and measure its characteristics? There are no direct ways for measuring properties such as the density, temperature or impurity content of such hot matter. Only indirect methods can be used for determining plasma properties through other measurable physical parameters — consequential effects caused by the plasma property in question. Developing methods for studying hot plasmas has evolved into an independent branch of plasma science called high-temperature plasma diagnostics. Diagnostics techniques often involve mathematical inverse problems, which are sometimes ill-posed and therefore need special algorithms for their solution. Several diagnostic methods developed recently for fusion-plasma research were originally developed in other contexts, for example X-ray and microwave spectroscopy in astrophysics, or neutron and gamma-ray detection in particle physics. Some diagnostic techniques were developed in the context of fusion plasmas, for example ion-temperature measurements using the energy spectra of hot neutral atoms escaping the plasma and born from plasma ions in charge-exchange reactions, or charge-exchange recombination spectroscopy, based on the analysis of the light emitted by plasma impurity ions in recombination reactions.

Let us illustrate how challenges in fusion research have led to progress in diagnostics by describing in more detail one of the methods developed specifically for fusion research, the heavy-ion beam probe (HIBP). This diagnostic technique for measuring the electric potential in the plasma core was invented in 1970s in the US and subsequently deployed in fusion machines all over the world[7]. The HIBP functions as follows (see Fig. 2). A primary beam of heavy ions with kinetic energy E_b, current I_b, mass m and charge number $q = 1$ (that is, with charge qe where e is the elementary charge) is injected into the hot plasma across the toroidal magnetic field B_t. The ions move along the Larmor circle with radius $R_L = (2mE_b)^{1/2}/qeB_t$. The probing beam passes through the plasma; beam ions collide with plasma particles, predominantly electrons, which leads to the formation of secondary ions with $q = 2$. These secondary ions move along Larmor circles with half the original radius, and form a fan of secondary orbits. The fan reaches a multi-slit analyser, located outside the plasma volume, which measures the detected energy E_d and current I of the secondary ions. In order for this to work, the Larmor radius of the ions should exceed the size of the plasma, which can be realized by using heavier ions with high energies. In modern devices, heavy ions such as Tl^+, Cs^+ or Au^+ are used, with

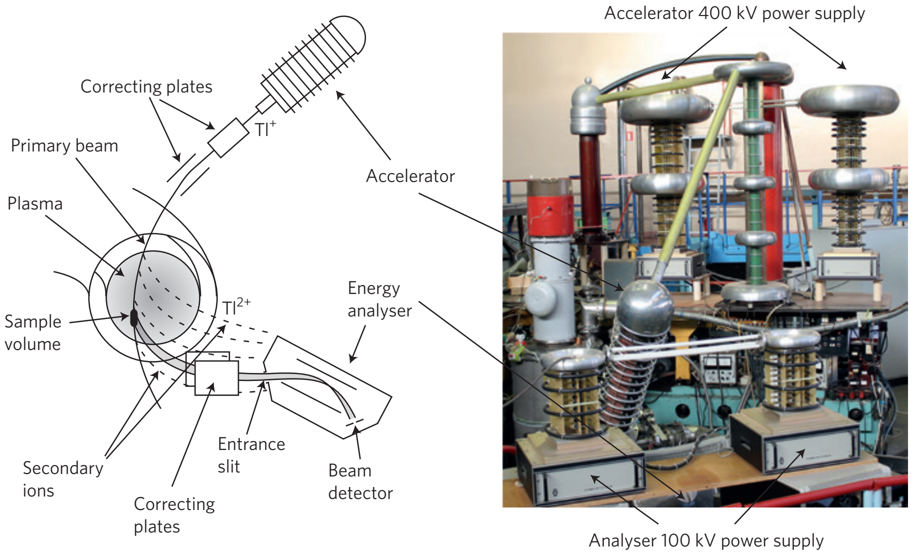

Figure 2 | Schematic of the working principle of a heavy-ion beam probe and photo of the corresponding hardware in the T-10 tokamak at the NRC 'Kurchatov Institute' (Moscow, Russia). Heavy ions (for example Tl^+) are accelerated and injected into the plasma, where they ionize again (Tl^{2+}), which halves their Larmor radius. If secondary ionization takes places in the region labelled 'sample volume', the ions will reach a multi-slit analyser, which measures the ions' energy and current. By varying the beam's entrance angle with respect to the plasma by means of correcting plates or by changing the beam's energy E_b through the power supply, the sample volume scans a plasma cross-section. Analysing the obtained data provides a wealth of quantitative information on various plasma parameters. Figure adapted with permission from ref. 27, MEPhI (schematic) and ref. 7, MEPhI (photo).

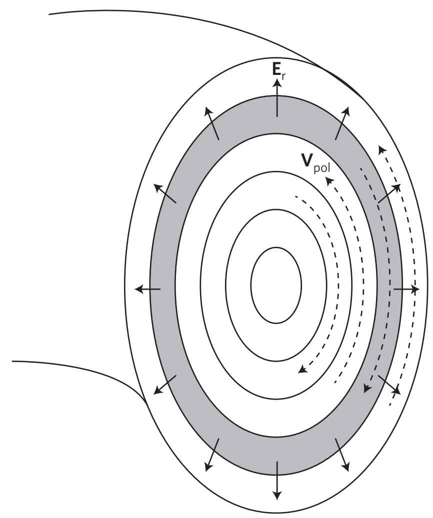

Figure 3 | Geodesic acoustic modes (zonal flow) in a magnetically confined plasma. Such modes are characterized by a radially localized, poloidally and azimuthally symmetric oscillating electrostatic potential, resulting in an oscillating radial electric field $\mathbf{E}_r$ (solid arrows), and hence in an oscillating poloidal flow with $\mathbf{V}_{pol} = \mathbf{E}_r \times \mathbf{B}_t$ (dashed arrows). The plasma potential and poloidal flow radial distributions are the experimentally accessible features. Figure adapted with permission from ref. 13, IOP.

beam currents up to tens of microamperes and energies of several hundreds of keV to MeV.

How can the plasma's electric potential ϕ be deduced from measurements of the secondary ions' energies E_d? The key idea is to exploit the principle of energy conservation. At the ionization point in the plasma, which is the HIBP sample volume, electrons with potential energy $-e\phi^{SV}$ are stripped off (ϕ^{SV} is the local electrostatic potential in the sample volume, which is typically below 1 cm^3). The kinetic energy E_d of a secondary ion leaving the plasma equals $E_b + e\phi^{SV}$. Hence, the plasma potential at the sample volume is given by $\phi^{SV} = (E_d - E_b)/e$. When varying the beam's angle of injection (and its energy), the ionization point scans the plasma, which allows ϕ to be determined at different points of the plasma cross-section.

The HIBP technique turned out to be applicable for measuring several other important plasma quantities too, such as the radial (E_r) and poloidal (E_{pol}) components of the electric field (particularly, oscillations of E_r and E_{pol}), the plasma drift velocity across the magnetic field $\mathbf{V}_r = \mathbf{E}_{pol} \times \mathbf{B}_t$, the electron density n_e (by measurement of the secondary beam current I), the radial turbulent particle flux $\Gamma_{\mathbf{E}\times\mathbf{B}} = n_e E_{pol}/B_t$ perpendicular to the magnetic field, and magnetic field oscillations in the plasma core (by measuring the beam's displacement ζ along the toroidal direction in the analyser)[8]. (It is important to note that all local data are averaged over the sample volume, the size of which hence determines the spatial resolution of the HIBP — a typical radial size for the sample volume is 0.1–1 cm.) Clearly, the HIBP is a multi-purpose diagnostics toolbox with which various properties of fusion plasmas can be studied[7].

New areas for fundamental research

As mentioned, although research on fusion plasmas has been mainly driven by the promise of energy production, new physical phenomena have been discovered along the way.

One example is the self-organization universally seen in hot toroidal plasmas, manifest in the constancy of the radial profile of the plasma pressure, regardless of the localization of the heat deposition or the type of heating source[9]. This phenomenon makes it evident that the conventional processes of diffusion and convection, as described by the diffusion equation, which are observed for solid, liquid and gaseous matter, are not applicable to magnetically confined fusion plasmas[10].

Another example is the discovery of zonal flows in fusion plasmas. Zonal flows constitute a universal mechanism for self-regulation of turbulence. The name originates from the stable atmospheric circulation along latitudinal lines in the Earth's atmosphere (jet streams), where zonal flows were first observed. They were later found to occur in the atmosphere of other planets of the Solar System too — the distinctive belts seen in Jupiter's atmosphere are a manifestation of zonal flows. These large-scale flows are formed through the merging of smaller-scale turbulence vortices.

In toroidal plasmas, zonal flows and their higher-frequency counterparts, geodesic acoustic modes (GAMs), were found as radially localized structures of a plasma's radial electric field component E_r or, equivalently, of the plasma's electrostatic potential ϕ. In the presence of a toroidal magnetic field B_t, such structures produce an oscillatory poloidal plasma rotation velocity $\mathbf{V}_{pol}$ at specific radii along the magnetic flux surfaces, given by $\mathbf{V}_{pol} = \mathbf{E}_r \times \mathbf{B}_t$. Zonal flows and GAMs look like large-scale vortices centred around

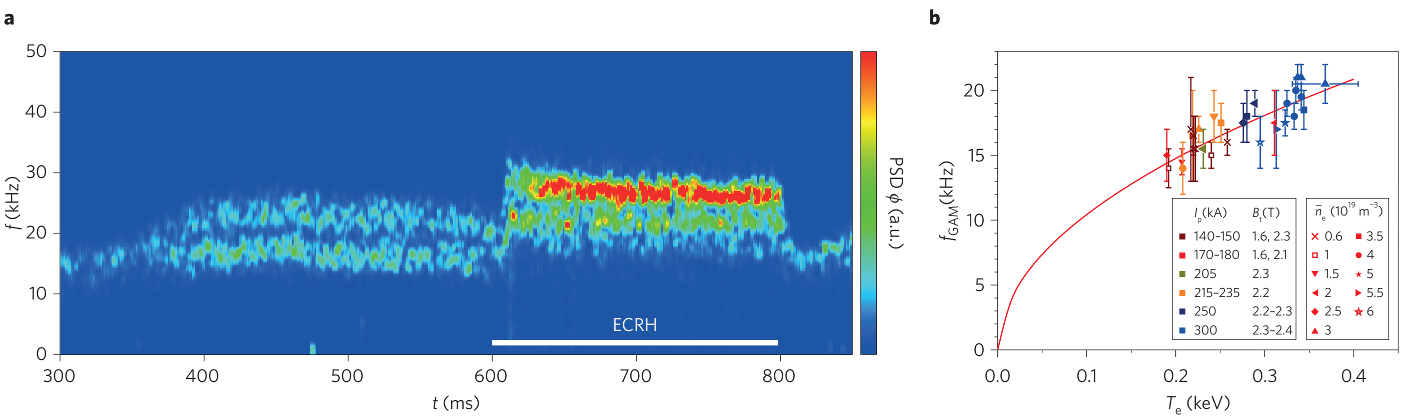

Figure 4 | GAMs in a magnetically confined plasma. **a**, Electric potential power spectrogram in the T-10 tokamak showing evidence of GAMs in the plasma discharge with auxiliary electron-cyclotron-resonance heating (ECRH). HIBP measurements are taken locally at normalized radius $\rho = r/a = 0.7$ (with r and a the radial coordinate and the minor radius of the plasma, respectively). The GAM frequency and power increase with increasing electron temperature T_e during the ECRH pulse; the GAM intermittent structure is clearly visible. PSD, power spectral density. **b**, Dependence of the GAM frequency on the local T_e at $\rho = 0.73$ in the T-10 tokamak. Data from several ohmically heated discharges with different plasma currents I_p, toroidal magnetic fields B_t and mean electron densities $\bar{n}_e$ display overall consistency with theoretical expectations. Figure adapted with permission from ref. 17, IAEA.

the plasma axis, as shown in Fig. 3. The energy source for zonal flows and GAMs is plasma micro-turbulence.

Owing to their poloidal direction, zonal flows and GAMs do not contribute to the energy and particle transport across the confining magnetic field **B**. Instead, they serve as a reservoir of free energy stored inside the confined plasma. But more importantly, this oscillatory rotation can suppress the plasma's micro-turbulence eddies by means of the $\mathbf{E}_r \times \mathbf{B}_t$ shearing mechanism, so zonal flows and GAMs can be considered as mechanisms of self-regulation of turbulence. Because plasma transport across the magnetic field does not display classical (collisional) but anomalous (turbulent) character, zonal flows and GAMs are relevant for studies of plasma confinement.

The occurrence of GAMs was predicted[11] in 1968, but only demonstrated experimentally in 2003 on the TEXT (Texas University[12]), DIII-D (General Atomics[13]) and T-10 (NRC 'Kurchatov Institute'[14]) tokamaks, through the application of advanced diagnostic techniques such as HIBP for measuring ϕ (ref. 15) and beam-emission spectroscopy for V_{pol} (ref. 13). GAMs can be seen in the power spectral density of plasma-potential oscillations, as a frequency peak with a dominating power having a high contrast with respect to the background turbulence (Fig. 4a). The temperature dependence of the GAM frequency can be calculated to be

$$f^{e}_{GAM} = \frac{1}{2\pi R}\sqrt{2T_e / m_i} \qquad (1)$$

where T_e is the local electron temperature, m_i is the plasma ion mass and R is the major radius of the torus[11]. This relation is crucial for correctly identifying GAMs in experiments (Fig. 4b). Although the local theory of GAMs[11] implies an increase in frequency with plasma temperature (that is, towards the centre of the plasma column), there is recent experimental HIBP evidence of a constant GAM frequency — in other words, of GAMs as global eigenmodes[16,17]. An advanced GAM-eigenmode theory has been put forward[18] but needs to be developed further.

A third example of a new area of fundamental physics research is that of Alfvén eigenmodes — electromagnetic waves in plasmas — originally discovered by Hannes Alfvén in the context of space plasmas in the 1940s. Alfvén waves propagate along magnetic field lines with a velocity $\mathbf{V}_A \propto \mathbf{B}_t n_e^{-1/2}$. In magnetically confined fusion plasmas, the structure of the magnetic field along the field lines is periodic, which can set up a resonance condition for Alfvén waves; from such resonances, Alfvén eigenmodes develop in toroidal plasmas[19].

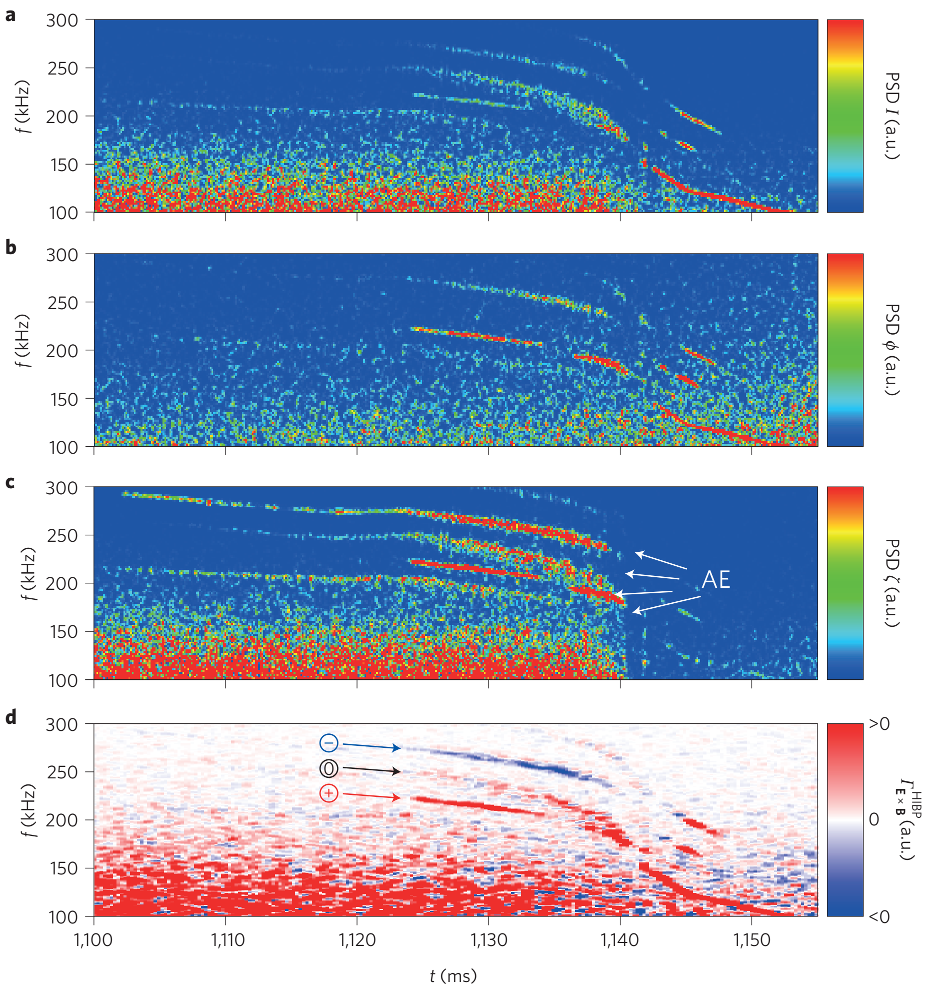

Figure 5 | Observation of Alfvén eigenmodes in an ECR- and NBI-heated discharge in the TJ-II stellarator (CIEMAT, Madrid, Spain). **a–c**, Time evolutions of the power spectral densities (PSD) obtained from HIBP measurements in the core plasma at mid-radius. Alfvén eigenmodes (AE) induced by neutral-beam injection are visible (labelled by arrows) as a set of monochromatic oscillations on the total secondary beam current I, proportional to n_e (**a**); the plasma electrostatic potential ϕ (**b**); the toroidal shift of the secondary beam ζ, proportional to B_{pol} (**c**). In this example, the Alfvén eigenmode frequencies are decreasing with time owing to the increase in density, according to the Alfvénic dependence on density, $f_A \propto V_A \propto n_e^{-1/2}$. **d**, The frequency-resolved turbulent particle flux $\Gamma_{\mathbf{E}\times\mathbf{B}}$: outward flux is in red, inward flux is in blue. The fact that the Alfvén eigenmodes are so pronounced in the flux spectral density function indicates that their contribution to the total turbulent flux is significant. Evidence of AEs producing outward (+), inward (−) and no (0) flux is indicated by red, black and blue arrows, respectively. Figure adapted with permission from: **a**, **b**, **c**, ref. 8, IAEA; **d**, ref. 21, IAEA.

Alfvén eigenmodes can be excited by the energetic particles injected when heating by means of neutral beam injection (NBI) or ion cyclotron resonance[20]. In future reactors, the alpha particles produced by fusion reactions will be the main energy source for Alfvén eigenmodes. The excitation of such eigenmodes may lead to extra losses of energetic and thermal particles from the bulk plasma, so it could potentially hamper the proper functioning of future fusion reactors such as ITER, where the heating by fusion alpha particles is crucial.

For studying electromagnetic waves in magnetically confined plasmas, direct measurements of oscillatory electric and magnetic fields inside the plasma column are necessary. The most direct diagnostic tool for such measurements is the HIBP because of its sensitivity to both magnetic and electrostatic oscillations[8]. An example of the observation of Alfvén eigenmodes in a stellarator plasma is given in Fig. 5a–c, showing the power spectra of plasma

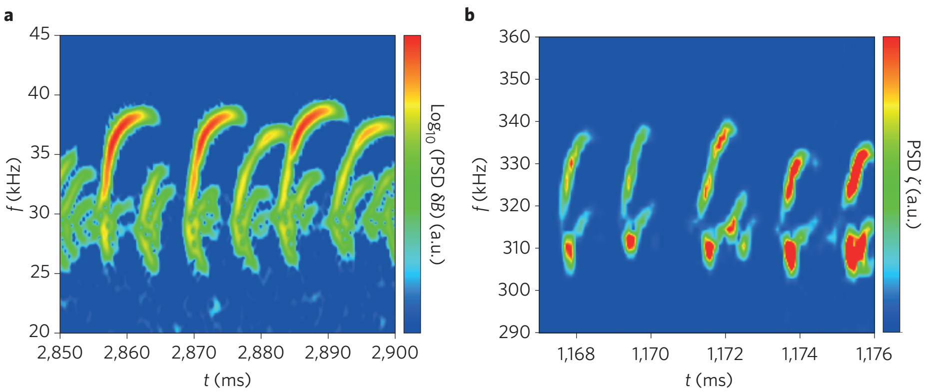

Figure 6 | Power spectral density (PSD) of the magnetic perturbations caused by chirping modes, excited by energetic particles in fusion plasmas. **a**, Magnetic-field perturbations (δB), measured by magnetic probes in the JET tokamak (Culham, UK), showing a toroidally symmetric e-GAM. **b**, Toroidal displacement of the probing beam (ζ), measured by HIBP in the TJ-II stellarator, showing an Alfvén eigenmode. The figure shows that the range of the mean frequency differs between **a** and **b** by an order of magnitude, and the range of the frequency variation during one cycle of chirping differs by a factor of 3. Furthermore the nature of the modes is also different. Nevertheless, one can see the remarkable similarity in the modes' frequency dynamics, which might be an indication that similar wave–particle interaction mechanisms, underlying the excitation and behaviour of the modes, are at play. Figure adapted with permission from **a**, ref. 22, IAEA; **b**, A.V.M. *et al.* (manuscript in preparation).

density, electric potential and magnetic field oscillations in a discharge with electron-cyclotron resonance and NBI heating. It is remarkable that each Alfvén eigenmode has its own individual characteristics in the HIBP power spectra; some of the modes have only a magnetic component, but no electrostatic component, whereas others have pronounced peaks in the magnetic, electrostatic and density spectra. The corresponding frequency-resolved turbulent particle flux is shown Fig. 5d. The flux related to broadband turbulence has an intermittent character; it consists of a series of stochastic bursts, which are mostly directed outwards. On top of the broadband turbulence are various Alfvén eigenmodes with different features. Most of the modes contribute to outward flux, some modes produce inward flux, some of the Alfvén eigenmodes produce no flux at all[21]. Typically, the Alfvén eigenmode contribution to the frequency-resolved turbulent particle flux is found to constitute a significant fraction of the total flux $\Gamma_{E\times B}$ This is an important topic of study in view of the plasma performance in ITER, as this is heated by energetic fusion alpha particles[19].

More fundamentally, the observation of modes in fusion devices shows that Alfvén waves are an intrinsic phenomenon in magnetized plasmas, occurring in both space and laboratory plasmas.

It is worth mentioning that experiments performed recently at the world's largest tokamak, the Joint European Torus (JET) in Culham, UK, show that GAMs present the lower-frequency limit for Alfvén eigenmodes[22]. It was also found that GAMs may be induced not only by plasma micro-turbulence, but also by fast particles, just as for Alfvén eigenmodes, that form 'energetic GAMs' or 'e-GAMs'. Both Alfvén eigenmodes and GAMs may exist not only in the conventional form of monochromatic oscillations but also in the form of the 'chirping mode' — a sequence of individual bursts with fast frequency changes. Figure 6 shows a chirping-mode e-GAM in JET[22] and a chirping-mode AE in the TJ-II stellarator (A.V.M. *et al.*, manuscript in preparation) manifesting themselves in associated magnetic field perturbations observed by means of magnetic probes and HIBP, respectively.

Concluding remarks

The above examples should make it clear that fusion research, originally driven by a clear applied goal, has also opened up wide fields of fundamental plasma physics and diagnostics research. Another aspect is the connection between astrophysical and laboratory magnetically confined plasmas, as nicely illustrated by the two phenomena discussed above: GAMs/zonal flows, originally discovered in the atmosphere of planets, and Alfvén waves, originally observed for space plasmas, have now not only been observed in fusion laboratory plasmas, but also found to be related. As we approach the plasma conditions for future fusion reactors such as ITER, we can expect further broadening of the fundamental research involved. In support of ITER, for which the understanding of mechanisms of plasma energy confinement constitutes a challenging open problem, machines under construction or being upgraded are oriented to the exploration of various promising ways towards better confinement: JT-60SA (ref. 23) and T-15 (ref. 24) focus on high toroidicity a/R, where a and R are the tokamak minor and major radii respectively, and high B_t, whereas the Wendelstein 7-X (W7-X) stellarator[25], which has just started operation, has a three-dimensional optimized magnetic configuration. Comprehensive studies of the plasmas in general, and their turbulence in particular[26], in these new machines present a great challenge for fundamental plasma physics and high-temperature plasma diagnostics.❐

Alexander V. Melnikov is at the National Research Centre 'Kurchatov Institute', 12382 Moscow, Russia, and the National Research Nuclear University MEPhI, 115409 Moscow, Russia.
e-mail: Melnikov_AV@nrcki.ru

References

1. Ongena, J., Koch, R., Wolf, R. & Zohm, H. *Nature Phys.* **12,** 398–410 (2016).
2. Shafranov, V. D. *Phys. Usp.* **44,** 835 (2001).
3. Peacock, N. J. *et al. Nature* **224,** 488 (1969).
4. Interview with Bernard Bigot. *Nature Phys.* **12,** 395–397 (2016).
5. Cowley, S. C. *Nature Phys.* **12,** 384–386 (2016).
6. Knaster, J., Moeslang, A. & Muroga, T. *Nature Phys.* **12,** 424–434 (2016).
7. Melnikov, A. V. *Electric Potential in Toroidal Plasma Devices* [in Russian] (MEPhI, Moscow, 2015).
8. Melnikov, A. V. *et al. Nucl. Fusion* **50,** 084023 (2010).
9. Esipchuk, Yu. V. & Razumova, K. A. *Plasma Phys. Control. Fusion* **28,** 1253 (1986).
10. Dnestrovskij, Yu. N. *Self-organization of Hot Plasmas* (Springer, 2015).
11. Winsor, N., Johnson, J. & Dawson, J. *Phys. Fluids* **11,** 2448 (1968).
12. Schoch, P. M. Connor, K. A. Demers, D. R. & Zhang, X. *Rev. Sci. Instrum.* **74,** 1846 (2003).
13. McKee, G. R. *et al. Plasma Phys. Control. Fusion* **45,** A477–A485 (2003).
14. Melnikov, A. V. *et al. Proc. 30th EPS Conf. Contr. Fusion and Plasma Phys.* ECA Vol. 27A, 3.114 (ECA, 2003).
15. Melnikov, A. V. *et al. Plasma Phys. Control. Fusion* **48,** S87 (2006).
16. Ido, T. *et al. Plasma Phys. Control. Fusion* **48,** S41 (2006).
17. Melnikov, A. V. *et al. Nucl. Fusion* **55,** 063001 (2015).
18. Ilgisonis, V. I. *et al. Plasma Phys. Control. Fusion* **56,** 035001 (2013).
19. Heidbrink, W. W. *Phys. Plasmas* **15,** 055501 (2008).
20. Mazon, D., Fenzi, C. & Sabot, R. *Nature Phys.* **12,** 14–17 (2016).
21. Melnikov, A. V. *et al. Nucl. Fusion* **52,** 123004 (2012).
22. Berk, H. L. *et al. Nucl. Fusion* **46,** S888 (2006).
23. Di Pietro, E. *et al. Fusion Eng. Design* **89,** 2128–2135 (2014).
24. Melnikov, A. V. *et al. Fusion Eng. Design* **96–97,** 306–310 (2015).
25. http://www.ipp.mpg.de/14226/top_news (7 April 2016).
26. Fasoli, A. *et al. Nature Phys.* **12,** 411–423 (2016).
27. Strelkov, V. S. *Physical Basis of Plasma Diagnostics Methods in Tokamak* [in Russian] (MEPhI, Moscow, 2004).

Acknowledgements

This study was exclusively financially supported by the Russian Science Foundation, project 14-22-00193. I acknowledge the long-term collaboration between NRC 'Kurchatov Institute', Russia, Kharkov Institute of Physics and Technology, Ukraine, and CIEMAT, Spain and the joint HIBP team.